Collective dynamics in glasses and its relation to the low-temperature anomalies

Andreas Heuer
Max-Planck-Institut für Polymerforschung, Ackermannweg 10, D-55128 Mainz, Germany

Robert J. Silbey
Massachusetts Institute of Technology, Cambridge, Massachusetts 02139
(Received 5 July 1995)

We present a systematic analysis of the low-temperature properties of glasses. In a first step we derive the low-temperature Hamiltonian of Lennard-Jones (LJ) glasses by a combination of numerical and analytical methods from first principles. This enables us to calculate the density of tunneling states, the coupling between tunneling states and phonons (deformation potential), and the extrema of $C(T)/T^3$ [$C(T)$ specific heat] for LJ glasses as functions of the velocity of sound, the density, and the glass transition temperature. In a second step we directly apply these results to more general glasses. Comparing the predictions for the four low-temperature parameters with experiment for a variety of glasses allows us to judge the degree to which their quantitative values are dominated by the individual microscopic structure. The agreement is excellent for the extrema of the specific heat and reasonable for the density of tunneling states and the deformation potential. Furthermore, we show from scaling arguments that such an agreement cannot be found for the peak of the sound absorption. From our simulations we can correlate the different degree of universality of the low-temperature observables with the different spatial extension of the relevant low-temperature excitations. In agreement with intuition, distinct collective dynamics translates into a weak dependence on the microscopic structure.

I. INTRODUCTION

One of the most fascinating aspects of the physics of glasses is their universal behavior at low temperatures. It is significantly different from that of their crystalline counterparts.[1] For example, most glasses show an approximately linear temperature dependence of the specific heat for very low temperatures ($T<1$ K), which has been explained by phenomenological models. The standard tunneling model (STM) (Refs. 2, 3) and, more recently, the soft potential model (SPM) (Refs. 4–7) postulate that at low temperatures the Hamiltonian of a glass can be decomposed according to

$$\mathscr{H}=\mathscr{H}_{\mathrm{SM}}+\mathscr{W}+\mathscr{H}_B\,, \tag{1}$$

where the first term describes localized excitations (*soft modes*) of the glass, the second term the interaction between soft modes and phonons, and the third term the phonon bath. Two temperature regimes may be distinguished at low temperatures. Taking the specific heat $C(T)$ as an example, for very low temperatures (typically $T<1$ K, regime I) one observes a linear temperature dependence. For higher temperatures (typically 1 K$<T<$10 K, regime II) $C(T)$ increases dramatically so that even $\hat{C}(T)=C(T)/T^3$ increases. Hence between regime I and regime II $\hat{C}(T)$ displays a minimum. For still larger temperatures $\hat{C}(T)$ decreases again. The two regimes are related to different types of soft modes. In regime I, where only low-energy excitations contribute, it is postulated that the relevant excitations can be described by doublewell potentials (DWP's) in the configurational space. This means that the units of the glass can switch between two adjacent minima of the potential energy. If, by chance, the corresponding DWP happens to be nearly symmetric the energy difference of the two lowest eigenstates is mainly dominated by the tunneling splitting and hence may be very small. In regime II the specific heat is dominated by excitations of singlewell potentials (SWP's) that correspond to localized rearrangements with very low restoring forces.

Note that the temperature dependence of the specific heat is directly related to the so-called Boson peak measured by Raman scattering.[8] Hence the results, presented below, are also relevant for understanding the microscopic origin of the Boson peak.

A different feature, also related to the existence of DWP's, is the sound absorption peak which is observed around 20–50 K.[9,10] It is typically explained via thermally activated relaxation processes of the DWP's.

In this paper we will deal with two basic questions related to the low-temperature properties: (i) What is the microscopic basis for the phenomenological models mentioned above and hence for the decomposition of the total Hamiltonian according to Eq. (1)? (ii) Do the low-temperature properties depend on the specific microscopic structure of the glass which, of course, substantially varies among different glasses? Both questions are basically equivalent to those put forward by Phillips at the end of his review article. He doubted that there would be a single theory answering these questions.[1] The present discussion will be based on the typical low-temperature parameters determined experimentally, namely the density of DWP's n_{eff}, the coupling constant γ between DWP's and the heat bath (we call them both *tunneling parameters*), and the temperatures $T_{C,1}$ and $T_{C,2}$ where $\hat{C}(T)$ displays a minimum and a maximum, respectively. Furthermore we will briefly discuss the temperature T_s, for which the acoustic absorption displays a maximum.

Due to the complexity of the problem no analytical theory for general glasses exists which fully derives the above decomposition of $\mathscr{H}$ on the basis of the original Hamiltonian

of the glass and which might thus provide a check of the assumptions of the phenomenological models. Only for special cases like a one-dimensional model glass were analytical calculations of the low-temperature properties possible.[11,12] Generally one is restricted to computer simulations of model glasses. It has been shown by Schober and co-workers[13–15] that glasses may contain localized low-frequency soft modes which correspond to the SWP's postulated in the SPM. The present authors were able to perform the above decomposition of the Hamiltonian for a Lennard-Jones (LJ) type model glass in the tunneling regime.[16] In this reference basic results of this analysis can be found. A detailed description of this decomposition and some specific results which are relevant for the subsequent parts are given in Sec. II.

Monatomic LJ glasses are characterized by three parameters, defining the mass, the energy, and the distance scale. Conveniently, this set of three parameters can be chosen as the mass m of the individual atoms, the average phonon velocity v, and the density ρ. Therefore, in principle it should be possible to express $\mathscr{H}_{\rm SM}$, $\mathscr{W}$, and $\mathscr{H}_B$ and hence all low-temperature properties as functions of (m,v,ρ). In Sec. III we will derive the quantitative relations connecting the four low-temperature parameters $n_{\rm eff}$, γ, $T_{C,1}$, $T_{C,2}$ with the material constants (m,v,ρ).

Question (ii) deals with the reason for the variation of the low-temperature parameters among different glasses. For example the deformation potential of SiO_2 is five times as large as that of polystyrene (PS). In principle this can be explained in two different ways. First, due to the significant microscopic differences between the two glasses, the observables of both glasses have nothing in common so that the observed ratio of five for the deformation potential is just an accident. However, there might be a different explanation. Let us for the moment consider the melting point of different noble gases. The fact that the melting point varies quite significantly can be explained by different internal energy scales (i.e., the interaction strength between two noble gas atoms). This variation directly translates into a variation of the melting temperature. Since the internal energy scale can be determined by other means (e.g., by analysis of the velocity of sound) one can predict the relative melting temperatures for different noble gases. With this example in mind one might ask whether the large differences among the low-temperature parameters can be related to different internal energy scales (and/or mass scales and/or distance scales) rather than to the microscopic differences. Whether nature prefers the first or second option can be checked rather easily. First we simply postulate that all glasses behave as LJ glasses. This assumption enables us to predict the low-temperature parameters for all glasses. We then check whether the predictions are consistent with experimental results. Possible deviations are a measure for the importance of the microscopic structure which, of course, is not well represented by a LJ type glass. We find that the agreement is excellent for the extrema of $\hat{C}(T)$ and reasonable for the tunneling parameters. However, we show that the temperature of the peak of sound absorption T_s does not follow a scaling relation. This behavior is in agreement with the well-known experimental fact that the peak of sound absorption is much more sensitive to microscopic changes [i.e., wetting of B_2O_3 (Ref. 17)] than the other low-temperature observables. This analysis is contained in Sec. IV.

The universal behavior at phase transitions is related to the diverging correlation length which averages out all microscopic differences.[18] The spatial extensions of different soft modes are rather small (1–50 atoms).[14,19] In Sec. V we show that properties which are related to more extended soft modes nevertheless display a weaker dependence on the microscopic structure. We finish with a brief summary in Sec. VI.

II. LOW-TEMPERATURE DECOMPOSITION OF THE HAMILTONIAN OF A MODEL GLASS

In this section we determine $\mathscr{H}_{\rm SM}$, $\mathscr{W}$, and $\mathscr{H}_B$ for a model glass which is similar to the one analyzed by Weber and Stillinger.[20] It is a diatomic LJ type glass for which the pair potentials are given by

$$V_{kl}(r)=A_{kl}[(\alpha_{kl}r)^{-12}-1]\exp[(\alpha_{kl}r-a_c)^{-1}],0<\alpha_{kl}r\leqslant a_c$$
$$=0,\quad \alpha_{kl}\geqslant a_c, \tag{2}$$

where $k,l\in\{1,2\}$ describe which pair of atoms is considered. 80% type I and 20% type II atoms are taken. The cutoff distance a_c is given by $a_c=1.652\sigma$, where σ is the unit length. Values for the potential parameters are $A_{12}=1.5A_{11}$, $A_{22}=0.5A_{11}$, $\alpha_{11}=1$, $\alpha_{12}=1.05$, $\alpha_{22}=1.13$. The parameters were chosen such that for $\sigma=2.2$ Å and $A_{11}=8200$ K the model glass is a good representative for an amorphous nickel phosphorus mixture. All simulations were performed at constant density of $\rho=8350$ kg m^{-3}. Periodic boundary conditions have been implemented. Simulation boxes with $N=150$ and 500 particles have been used. The total Hamiltonian of the glass reads

$$\mathscr{H}=\sum_{i=1}^{N}\frac{m_i}{2}\left(\frac{d}{dt}\vec{r}_i\right)^2+\sum_{i<j}V_{\eta(i)\eta(j)}(r_{ij}), \tag{3}$$

where $\vec{r}_i$ denotes the position vector of particle i, r_{ij} the distance between particles i and j, m_i the mass of particle i, and $\eta(i)=1,2$. In what follows all three terms $\mathscr{H}_{\rm SM}$, $\mathscr{W}$, and $\mathscr{H}_B$ will be described on a microscopic basis.

A. Material constants

We first express the average velocity of sound v and the density ρ in terms of the microscopic parameters defining the model glass. In Ref. 21 we derived that to a good approximation

$$mv^2=\frac{2n}{51}f^{(2)}a^2, \tag{4}$$

where $f^{(2)}$ describes the second derivative of the pair potential at its minimum a. The average sound velocity v is defined as $3v^{-3}=v_l^{-3}+2v_t^{-3}$ where v_t and v_l are the transverse and longitudinal sound velocity, respectively. Equation (4) has been derived for a monatomic system but can be simply generalized to a multicomponent system if we use the average mass and the average value of $f^{(2)}a^2$. Summing over the three different pairs of atoms with the appropriate statistical weight yields $f^{(2)}a^2=91\,000$ K in the case of NiP. For m we have $m\approx 56m_p$. For the potential given above we have

$a=1.1\sigma$. n describes the number of atoms in the nearest neighbors shell, hence $n=12$ for NiP. Since we want to generalize our results to glasses with different values of n we will calculate all quantities for general n. Evaluation of Eq. (4) for NiP yields $v=2530\ \mathrm{ms}^{-1}$ which compares very well with the experimental value of $v=2600\ \mathrm{ms}^{-1}$.[20]

B. Soft modes

As a first step, we systematically search for DWP's in a given glass configuration which we obtain by quenching an equilibrated computer liquid. The principle goal is to find nearby configurations which both correspond to local energy minima. For a monatomic LJ type glass an appropriate measure for the distance between two configurations is the Euclidian distance

$$\mathrm{dist}(\{\vec{r}_{i,L}\},\{\vec{r}_{i,R}\})\equiv\sqrt{\sum_i(\vec{r}_{i,L}-\vec{r}_{i,R})^2}. \tag{5}$$

Furthermore we define the vectors $\vec{d}_i$ via $\vec{d}_i\equiv\vec{r}_{i,L}-\vec{r}_{i,R}$ and $d\equiv\mathrm{dist}(\{\vec{r}_{i,L}\},\{\vec{r}_{i,R}\})$ where $\{\vec{r}_{i,L}\}$ and $\{\vec{r}_{i,R}\}$ correspond to the left and the right glass configuration, respectively. In general, the transition between two minimum configurations involves the motion of all particles. Hence one has to look in the high-dimensional space to locate possible DWP's.

Recently, we presented an algorithm which for the first time systematically finds DWP's on a microscopic basis.[16] We start from one randomly selected atom and its $s\approx15$ nearest neighbors and analyze by appropriate variation of the positions of the $s+1$ atoms in which direction of the $3(s+1)$- dimensional configurational subspace an adjacent minimum of the potential energy may be localized. Based on this information we then check by variation of the positions of all atoms whether or not a second minimum can indeed be found. This procedure is repeated for all atoms and finally for different initial configurations. A closer description of the algorithm can be found in Ref. 16. We located approximately 300 DWP's with $d<a$ and $|A|$, $V<400$ K. It turned out that there exists approximately 1 DWP per 100 atoms. Of course, it is principally impossible to judge whether we determined all DWP's in this parameter range. Nevertheless it is possible to draw some indirect conclusions about this question. They will be presented further below.

For every DWP we parametrize the reaction path between the two minima of a DWP with the variable x, such that for $x=0$ the system is in the left well and for $x=d$ in the right well. The Hamiltonian of this one-dimensional subsystem reads

$$H_{\mathrm{DWP}}=\frac{m}{2}\left(\frac{d}{dt}x\right)^2+E_{\mathrm{pot}}(x), \tag{6}$$

where $E_{\mathrm{pot}}(x)$ describes the DWP with minima at $x=0$ and $x=d$. Note that all properties of the DWP are included in E_{pot} (e.g., the number of atoms participating during the motion). In addition to d, the DWP is determined by its asymmetry A and its potential height V. In practice it turns out that for the determination of V it is essential to determine the saddle point between both minima. Nearly all DWP's, found by this algorithm, have asymmetries much larger than 1 K and hence do not contribute to the low-temperature anomalies. Due to the strong correlations among the three parameters (e.g., DWP's with large asymmetries typically have large potential heights) it is not possible to directly extract reliable information about nearly symmetric DWP's.

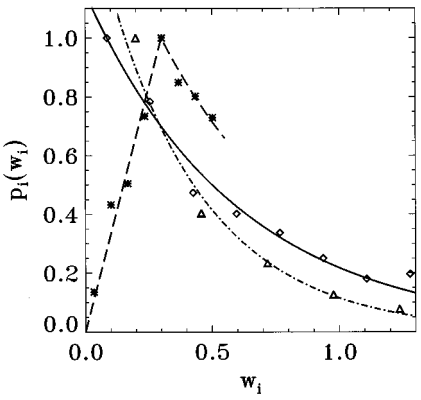

FIG. 1. The distribution $p_i(w_i)$ as determined from the analysis of the DWP's and a fit specified in Eq. (9) (stars: $i=2$; diamonds: $i=3$; triangles: $i=4$).

This problem can be circumvented by parametrizing the DWP's according to

$$E_{\mathrm{pot}}(x)=B\cdot[w_2(x/a)^2-w_3(x/a)^3+w_4(x/a)^4], \tag{7}$$

with $B\equiv mv^2$. The triplets (w_2,w_3,w_4) are defined by the values of A, V, and d. Choosing both minima of a DWP as $x=0$ we obtain two triplets per DWP. The above parametrization is motivated by the soft potential model which uses a similar parametrization although it is often the maximum of the DWP which is chosen as $x=0$. Via a statistical analysis which is also described in Ref. 16 we showed that, to a good approximation, the total distribution $p_{\mathrm{total}}(w_2,w_3,w_4)$ of DWP's factorizes as

$$p_{\mathrm{total}}(w_2,w_3,w_4)\approx p_2(w_2)p_3(w_3)p_4(w_4), \tag{8}$$

where the p_i are the distribution functions of the w_i. Due to this factorization it is now possible to obtain statistical reliable information about the regime of nearly symmetric DWP's. Note that the determination of the p_i is somewhat involved since one only has information about the subspace of soft modes which form DWP's.[16] The numerically determined distribution functions p_i are displayed in Fig. 1. To a very good approximation the p_i can be approximated as

$$\begin{aligned}p_2(w_2)&\propto(w_2/A_2)\Theta(A_2-w_2)\\&\quad+\Theta(w_2-A_2)\exp[-(w_2-A_2)/2A_2],\\p_3(w_3)&\propto\exp(-w_3/A_3),\\p_4(w_4)&\propto\exp(-w_4/A_4),\end{aligned} \tag{9}$$

with $A_2=0.30$, $A_3=0.60$, and $A_4=0.39$. Note that initially we did not restrict the p_i to be of any specific form. The distribution functions p_i and hence the A_i slightly depend on the discretization chosen for the w_i axis. The variance of the A_i allows us to estimate that the statistical error of A_2 and A_4 is of the order of 20%. The error of A_3 is somewhat larger since DWP's typically have large values of w_3 so that the determination of p_3 for small values of w_3 has a larger statistical

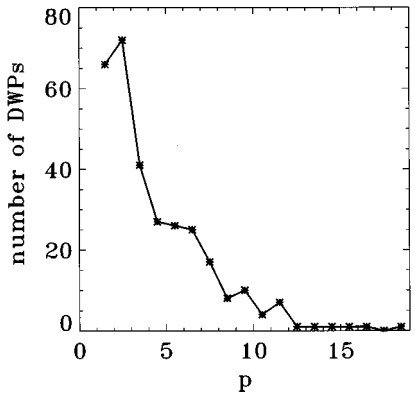

FIG. 2. The distribution of the effective mass p.

error. Furthermore the number of DWP's with very large values of w_2 is also very small since soft modes with large values of w_2 tend to form single well potentials. Therefore the nature of the final decrease of p_2 with w_2 can only be estimated qualitatively.

There are some characteristic features which elucidate the microscopic nature of the DWP's. The first point concerns the effective mass p of the DWP's. p is defined as d^2/d_k^2 where k denotes the number of the particle which moves most. In the limit that only a single particle moves we have $p=1$. In Fig. 2 we present the distribution of p. The average value of p is approximately 4. Hence collective dynamics is important to explain the microscopic nature of the DWP's. However, the DWP's can still be regarded as very localized excitations. For two-dimensional LJ glasses the general properties of DWP's have been recently published.[22] By comparing results from the simulations of $N=150$ to those of $N=500$, we checked that the absolute number of DWP's and the distribution of the effective mass do not depend on the size of the box.

The question arises whether the potential parameters are connected to the size of the DWP, hence to the value of p. The dependence of the average values of w_i on p is shown in Fig. 3. In a first approximation typical values of w_i are inversely proportional to p. Qualitatively this result is not surprising. In the limit that p is small the environment of a DWP is very stiff and hence typical energies involved in the

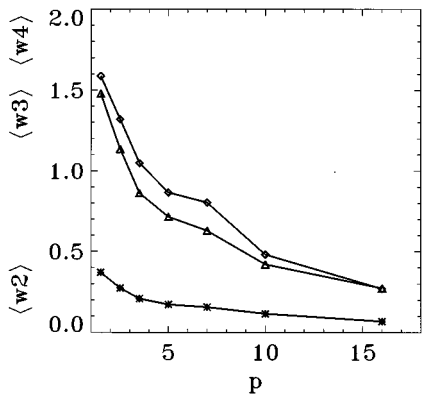

FIG. 3. The dependence of the average values w_i on the effective mass p.

transition between the two energy minima tend to be rather large. This result is essential in understanding the universal behavior of glasses presented below. On first sight it might seem surprising that, e.g., typical values of $\langle w_4\rangle$ are of the order of one whereas A_4 is less than 0.5. One reason for this apparent contradiction is that there exist a few DWP's with very large values of w_4 which are not captured by the exponential function $\exp(-w_4/A_4)$. The occurrence of such DWP's somewhat increases the average value of w_4. Furthermore one has to keep in mind that the distribution $p_4(w_4)$ does not directly represent the number of DWP's with some specific value w_4 (see the discussion above).

Another property concerns the relative motion of the different particles during the transition. Let us consider the expression

$$\chi=\sum_{i<j}{}' \frac{(\vec{d}_{ij}\cdot\vec{r}_{ij,0})^2}{r_{ij,0}^2}, \tag{10}$$

with $\vec{r}_{ij}\equiv\vec{r}_i-\vec{r}_j$ and $|\vec{r}|\equiv r$ for all vectors $\vec{r}$. The index 0 denotes the intermediate configuration which is defined as the average over the left and the right configurations. The prime indicates that the sum only extends over nearest neighbors. This expression checks whether the relative motion of two particles is correlated to their relative direction. In case that no correlation exists one would expect $\chi=\Sigma'_{i<j}(d_{ij}^2/3)$. We evaluated the value of χ for our DWP's. Interestingly it turned out that the value was approximately 60% smaller than expected for the uncorrelated case. Hence the relative motion of two near neighbor particles tends to be perpendicular to their relative position vector. The effect of this correlation is to minimize the change in distance and hence in potential energy between nearest neighbors.

In Ref. 13 the time evolution of a soft sphere glass has been determined via a molecular dynamics (MD) simulation. The authors report to have detected a few DWP's with effective masses which on average are twice as large as the effective masses determined from our simulations. This discrepancy might be a result of the different simulation method. A MD simulation can only detect DWP's for which the barrier height is of the order of k_BT. Hence for low-temperature simulations only DWP's with very small potential heights are detected. On the basis of our observation that DWP's with small energy scales tend to have larger effective masses it is plausible that the MD simulation overestimates the average effective mass of DWP's. Furthermore the two minima of a DWP detected during the MD simulation may be quite far apart in configuration space whereas we restricted ourselves to $d<a$. It is reasonable to assume that DWP's with large values of d have larger effective masses, hence giving a further possible explanation for the observed discrepancy.

For $w_2w_4>32/9$, w_3^2, $E_{\rm pot}(x)$ describes a SWP. *A priori*, no definite statements can be made about the distribution and absolute number of SWP's. However, since all w_i are distributed independently in the DWP regime one is tempted to assume that DWP's as well as SWP's are described by the same distribution functions p_i. This assumption will be the basis for our analysis of the temperature dependence of the specific heat in regime II. The existence of localized low-frequency excitations in glasses has already been demonstrated numerically.[13–15] The effective masses were of the

order of 20 and hence larger than those we determined in the DWP regime. However, since we obtained the empirical relation that the typical effective mass p increases for decreasing w_i and hence for decreasing potential heights V it is not surprising that in the limit of vanishing values of V the average effective mass is significantly larger than in the DWP regime.

We briefly want to comment on the question to which degree we systematically find all DWP's in the parameter range specified above. A single DWP can in principle be found starting from different initial clusters. A necessary condition is that the initial cluster has a significant overlap with the central part of the DWP. The number of times a specific DWP is found by our algorithm may be used to judge how difficult it is to locate a DWP in the configurational space. It turned out that this number may vary between 1 and approximately 20. First we note that the fraction of DWP's which has only been found once or twice is rather small (less than 20%). This indicates that most DWP's are reliably found by the algorithm. Furthermore we checked whether the properties of the DWP's which were only found once or twice are different as compared to the average properties. First it turns out that the average value of p for this subensemble is approximately 20% larger than the average value for the whole ensemble. This is in agreement with intuition since DWP's with larger effective masses can be expected to be more difficult to locate. This effect is not dramatic so that we are confident that our numerical distribution of p in Fig. 2 is only slightly hampered. Furthermore it turns out that the average potential height of this subensemble is nearly identical to the average potential height of the whole ensemble. This observation is very promising since it indicates that the average energy scale of the DWP's which are hard to locate is similar to the energy scale of all DWP's. Hence we may conclude that even for the worst case that we missed a significant number of DWP's, the distribution of DWP's which we found by our algorithm is representative for all DWP's.

C. The coupling between soft modes and phonons

In the deformation potential approximation the interaction between a single soft mode and phonons can be written as

$$\mathscr{W}=\gamma_\sigma e s_z, \tag{11}$$

where e denotes the strain field of the phonon bath, $\sigma=l,t$ the polarization of the corresponding phonon, and $s_z=\pm 1$ whether the system is in the left or the right well.[1] For a DWP γ_σ can be calculated via

$$\gamma_\sigma=\frac{1}{2}\frac{\partial[\mathscr{H}_R-\mathscr{H}_L]}{\partial e}. \tag{12}$$

$\mathscr{H}_{L,R}$ describes the total Hamiltonian $\mathscr{H}$ around the left and the right energy minimum, respectively. We evaluated this formal expression for the DWP's we found by our simulation.[21] Since we observed a correlation of γ_σ with the distance d between the two minima our results can be expressed as

$$\gamma_\sigma=\Gamma_\sigma(d/a). \tag{13}$$

The prefactor Γ_σ can be related to the material constants via

$$\Gamma_l\approx\frac{B}{\sqrt{n}} \tag{14}$$

and

$$\Gamma_t\approx\frac{2B}{3\sqrt{n}}. \tag{15}$$

All relations have been obtained by averaging over a large number of DWP's. The individual values of $\Gamma_{l,t}$ may vary as much as a factor of approximately five between different DWP's.

Furthermore one can show that the deformation potential disappears if the intermediate configuration has icosahedral symmetry.[21] Therefore disorder is essential to enable interaction between a soft mode and the phonon bath.

III. DETERMINATION OF THE LOW-TEMPERATURE PARAMETERS FOR THE MODEL GLASS

Based on the low-temperature decomposition of the Hamiltonian of the glass presented above it is possible to calculate the low-temperature parameters of a LJ type glass for given glass parameters (m,v,ρ). For the calculation of $n_{\rm eff}$ (the density of DWP's per volume and per energy) and the deformation potential one has to integrate over the distribution of DWP's and calculate for every triplet (w_2,w_3,w_4) the eigenvalues of the corresponding Hamiltonian in Eq. (6) and the average deformation potential as given by Eq. (13). Incorporating our knowledge of the absolute number of DWP's it is then possible to estimate $n_{\rm eff}$ in a quantitative way. For NiP we obtain $n_{\rm eff}=1.6\times10^{46}\ {\rm J}^{-1}\,{\rm m}^{-1}$, $\gamma_t=0.25$ eV, and $\gamma_l=0.38$ eV. It turns out that all quantities depend mildly on energy and hence on temperature. The above values hold for $E=1$ K (for NiP) where E denotes the energy difference of the lowest two energy eigenvalues of the soft mode.

For the estimation of $T_{C,1}$ and $T_{C,2}$ one has to calculate the specific heat on the basis of the distribution of soft modes. In the limit that for all soft modes only the lowest two energy levels are kept the specific heat is given by the well-known expression[1]

$$C(T)=\sum_{\rm SM}\frac{E^2}{4k_BT^2}\cosh^{-2}(E/2k_BT). \tag{16}$$

It turns out that incorporation of higher energy levels does not influence the value of $T_{C,1}$, whereas $T_{C,2}$ is shifted downwards by approximately 10%. For NiP we numerically obtain $T_{C,1}=2.8$ K and $T_{C,2}=10.2$ K. Similar calculations with adjustable parameters have been already performed in Ref. 5 in the framework of the SPM. In our approach the values of $T_{C,1}$ and $T_{C,2}$ have been obtained without invoking any fitting routine. We also find that the temperature dependence of the specific heat only changes slightly if $p_4(w_4)=\exp(-w_4/A_4)$ is replaced by $p_4(w_4)=\delta(w_4-A_4)$. Therefore, for many practical purposes it is possible to skip the integration over w_4. Only for heat release experiments is the total distribution of w_4 relevant.[23]

So far we have discussed the low temperature parameters for a specific choice of (m,v,ρ). The question arises whether

TABLE I. The parameters $b_{i,\mathrm{exp}}$,c_i(sim) which were used for estimating the experimental data, the parameter $b_{i,\mathrm{sim}}$ as determined from our simulations, the exponent c_i(SPM) as calculated within the soft potential model and the deviations σ_i between estimated and experimental parameters for the deformation potential ($i=1$), the product $n_{\mathrm{eff}}\gamma^2$($i=2$), the minimum of $\hat{C}(T)$($i=3$), and the maximum of $\hat{C}(T)$($i=4$).

i	$b_{i,\mathrm{sim}}$	$b_{i,\mathrm{exp}}$	c_i(sim)	c_i(SPM)	σ_i
1	22	25	0.2	0.16	0.23
2	0.0035	0.003	0.4	0.5	0.43
3	0.008	0.011	2/3	2/3	0.14
4	0.027	0.033	0.5	0.5	0.08

it is possible to obtain general expressions relating the low temperature parameters to material constants. We will show that this can be achieved on the basis of rather simple dimensional arguments. Let $\mathcal{O}$ be a dimensionless observable. First, we note that $\mathcal{O}$ has to depend on dimensionless combinations of material constants. In the classical regime (e.g., at the glass transition) no dimensionless combination of the parameters v, m, and ρ exists, hence in that regime, $\mathcal{O}$ does not depend on material constants. This simple fact is equivalent to the law of corresponding states. However, this statement is no longer true in the quantum regime where observables may also depend on the Planck constant $\hbar$. Let us define the dimensionless quantity μ via

$$\mu \equiv (0.011B)^{8/3} v^{-10/3} \rho^{-2/3} \hbar^{-2}. \tag{17}$$

For the choice of the numerical factor 0.011 see below. Apart from numerical factors μ is the only dimensionless combination of $(m,v,\rho,\hbar)$. Therefore $\mathcal{O}$ may depend on the material constants only via μ. In order to determine the dependence of $\mathcal{O}$ on the material constants it is therefore sufficient to calculate the dependence on μ.

Combining the above arguments one can write for the low-temperature parameters ($k_B=1$)

$$\gamma_l = B n^{-1/2} f_1(\mu), \tag{18}$$

$$n_{\mathrm{eff}}\gamma^2 = \rho v^2 n^{-1} f_2(\mu), \tag{19}$$

$$T_{C,1} = B f_3(\mu), \tag{20}$$

$$T_{C,2} = B f_4(\mu), \tag{21}$$

with dimensionless functions $f_i(\mu)$. They can be determined by repeating the above calculations for NiP for different values of m and hence for different values of μ. For the μ values of interest we obtain, to a good approximation, $f_i(\mu) = b_{i,\mathrm{sim}} \mu^{-c_i}$. The c_i and $b_{i,\mathrm{sim}}$ are given in Table I.

At this point we would like to mention that the four exponents c_i given above can in principle also be obtained in the framework of the soft potential model with the standard assumptions that (i) $p_2(w_2)$ is linear in w_2 for small w_2 and finally levels off, (ii) $p_3(w_3)$ is constant, and (iii) $p_4(w_4)$ is a delta function for some value w_4^0. Apart from logarithmic corrections c_1 and c_2 can be estimated by analyzing the Jacobi determinants for the transformation to the tunneling parameters.[7] One obtains $c_1=1/6$ and $c_2=1/2$ which compares rather well with the results of our numerical analysis. Differences are due to the logarithmic corrections and the use of the more general distribution functions p_i. This similarity indicates that the values of the exponents are rather insensitive to the exact structure of the distribution functions and hence do not depend on the details of our numerical simulations. Let us briefly discuss the intuitive meaning of $c_1>0$. In the limit of large masses tunneling is only possible for small values of d. Since $\gamma \propto d$ the average value of γ decreases for larger masses, hence $c_1>0$.

For the discussion of the temperature dependence of the specific heat and hence of the energy distribution of soft modes it is important to realize that very low values of E can only occur via tunneling. Hence below some crossover energy E_1 the soft modes are dominated by DWP's. The minimum value of E for SWP's is obtained for $w_2=w_3=0$. The average value of w_4 is A_4. Solving the corresponding Schrödinger equation for this quartic potential one obtains that E_1 is proportional to $BA_4^{1/3}\mu^{-2/3}$,[7] hence $c_3=2/3$, again in good agreement with our numerical result. In the regime $E>E_1$ the density of SWP's and, correspondingly, the specific heat dramatically increase due to the linear increase of p_2. Since the distribution p_2 levels off around $w_2=A_2$ the strong increase of the density of SWP's slows down around $E=E_2$ yielding the maximum in $\hat{C}(T)$. The eigenvalue of the corresponding harmonic SWP is proportional to $A_2^{1/2}B\mu^{-1/2}$ yielding $c_4=1/2$ once more in agreement with our simulations.

Apart from the μ dependence the above analysis shows that the values of E_1 and E_2 and hence of $T_{C,1}$ and $T_{C,2}$ are insensitive to numerical uncertainties in A_2 and A_4. Furthermore we see that the value of A_3 does not enter the low-temperature parameters. However, it is easy to check that the number of DWP's relative to the number of SWP's depends on A_3. The smaller A_3 the larger is the relative number of DWP's. We will discuss this aspect further below.

In summary, we have succeeded in calculating the four low-temperature parameters for *all* LJ glasses. In contrast to the soft potential model which is able to predict the relative values of the low-temperature parameters for different glasses, we are able to estimate the absolute values. Unfortunately it is not possible to compare our data with experimental data on LJ systems, since these have a strong tendency to crystallize, hampering the determination of bulk low-temperature properties for nonmetallic LJ glasses. Therefore, we have to generalize our results to other glasses like silicate glasses or polymers in order to compare our predictions with a larger amount of experimental data.

IV. APPLICATION TO GENERAL GLASSES

The results presented above are valid for the set of all LJ glasses. The question arises to which degree the physics of the low-temperature properties depends on the microscopic nature of the glass. Let us simply assume that it does not depend on the microscopic structure at all, and then predict the low-temperature parameters of all glasses. Comparison with experimental data will reveal whether or not this assumption is reasonable.

For LJ glasses we expressed the low-temperature parameters in terms of the velocity of sound v, the density ρ, and

TABLE II. The experimental data and its references as used in this paper.

	ρ [kg m^{-3}]	T_g [K]	v [10^3 m s^{-1}]	γ_t [eV]	$n_{\text{eff}}\gamma_t^2$ [10^7 J m^{-3}]	$T_{C,1}$ [K]	$T_{C,2}$ [K]	n	Ref.
SiO_2	2200	1473	4.1	0.65	0.87	2.1	10	4	6, 27
Se	4300	304	1.17	0.14	0.1	0.7	3.1	6	27, 37
PMMA	1180	374	1.70	0.27	0.11		3.5	6	27, 37
PS	1050	355	1.67	0.13	0.12	0.9	3.4	6	27, 37
Epoxy	1200	350	1.66	0.22	0.14	1.0	3.7	6	27, 34
BK7	2510	836	4.19	0.65	1.19			4	27
As_2S_3	3200	444	1.69	0.17	0.15			6	27
LASF7	5790	957	3.95	0.92	0.87			6	27
SF4	4780	693	2.48	0.48	0.65			4	27
SF59	6260	635	2.13	0.49	2.8			4	27
V52	4800	593	2.51	0.52	4.9			6	27
BALNA	4280	520	2.59	0.45	4.8			6	27
LAT	5250	723	3.1	0.65	3.7			6	27
Zn glass	4240	570	2.58	0.38	3.6			6	27
PC	1200	418	1.86	0.18	4.1			6	27
$LiCl\cdot 7H_2O$	1200	139	2.5		7.2	3.3	10.7	6	6, 27
GeO_2	3600	830	2.6			2.1	8.1	4	6, 35
B_2O_3	1800	523	2.06			1.3	5.4	6	38, 39
PB	930	186	1.69			1.4	5.1	6	6, 38
$(SiO_2)_{0.75}(NaO)_{0.25}$	2440	735	3.5			3.5	13.5	4	36, 38

the mass of the elementary units m. Furthermore we estimated the influence of the coordination number n. Trivially for a LJ glass the elementary units are given by the individual atoms. For a more complex glass the elementary units are typically the molecular units. For some glasses the molecular units can be reliably identified. For example for SiO_2 the molecular units are the SiO_4 tetrahedra, since at low temperatures the tetrahedral structure is very stable whereas the tetrahedra are mobile with respect to each other. Unfortunately, for some glasses like, e.g., silicate blends it is hard to say which molecular unit should be taken in order to define a mass m. Recently, Heuer and Spiess have shown for a number of glasses that to a good approximation m can be related to the glass transition temperature T_g via $T_g = c_g m v^2$ with $c_g \approx 0.011$.[24] This criterion can be considered as a generalization of the Lindemann melting criterion.[25] Therefore we may alternatively express the dependence of the low-temperature parameters on (T_g, v, ρ), without resorting to the somewhat arbitrary choice of m. Hence for a given glass with parameters (T_g, v, ρ) we may calculate the low-temperature parameters under the assumption that it behaves like a LJ glass. Of course, we could have started from the very beginning with characterizing a LJ glass by (T_g, v, ρ) instead of (m, v, ρ). However, since the atomic mass is a more natural choice for LJ glasses we feel that it is helpful to show that these choices can be related via $T_g = c_g m v^2$ and hence the value of T_g is an excellent measure of the internal energy scale. It should be noted that the glass transition temperature is not a well defined value but depends for example on the cooling rate or on the molecular weight in the case of polymers.[26] However, these uncertainties are relatively small and can be neglected for our subsequent analysis. The only remaining uncertainty is the choice of n. We choose $n=4$ for tetrahedral glasses, $n=12$ for NiP, and $n=6$ elsewhere.

In what follows we compare the theoretical predictions with experimental data. The data and references we used are listed in Table II. The tunneling parameters are taken exclusively from the data collection in the work of Berret and Meissner.[27] We omitted the value of the deformation potential of LiCl-$7H_2O$ since this value is hard to access experimentally (see the discussion in Ref. 27). Furthermore we omit the data for the Se_xGe_{1-x} semiconductors. They will be discussed in Sec. V.

The result of the comparison with experimental data is presented in Figs. 4–7. In principle we could use the c_i and

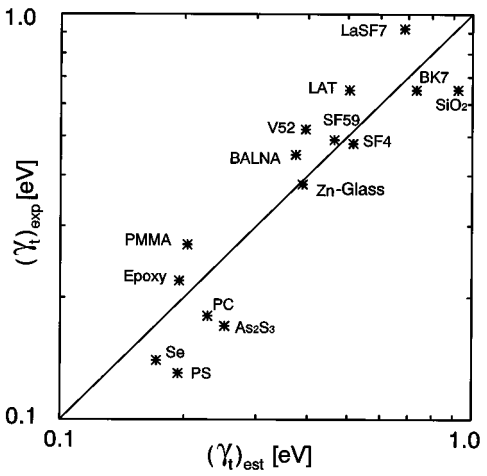

FIG. 4. A comparison of the estimated deformation potential and the experimental deformation potential. A single adjustable parameter has been used to scale the estimated data relative to the experimental data.

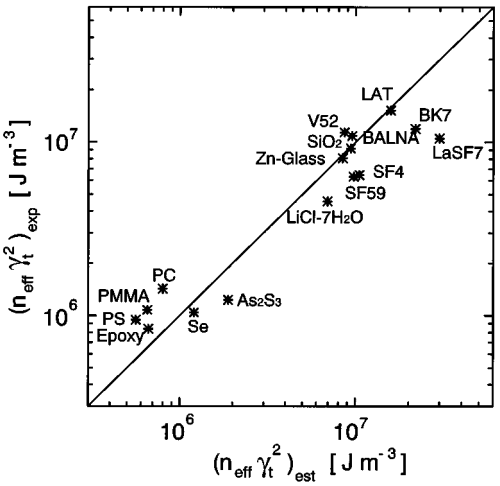

FIG. 5. The same analysis as in Fig. 4 for the density of tunneling systems.

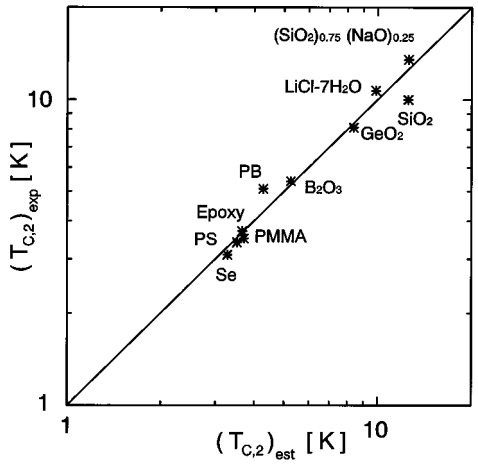

FIG. 7. The same analysis as in Fig. 4 for $T_{C,2}$.

$b_{i,\mathrm{sim}}$ as derived from our LJ glass analysis in order to predict the low-temperature parameters. For practical reasons we decided to treat the prefactors as adjustable parameters $b_{i,\mathrm{exp}}$. Of course, finally we have to check that $b_{i,\mathrm{sim}}$ and $b_{i,\mathrm{exp}}$ agree within reasonable limits. In order to quantify the scattering of the data we define the relative deviation σ_i as the average value of $|x_{i,\mathrm{sim}}-x_{i,\mathrm{exp}}|/x_{i,\mathrm{exp}}$ where x_i denotes the corresponding low-temperature parameter. The results for the fitted proportionality constants $b_{i,\mathrm{exp}}$ and the average relative deviations σ_i are also listed in Table I.

For all four quantities significant correlations can be observed. Hence one can already conclude that the individual microscopic structure does not dominate the actual low-temperature behavior. From the σ_i values it is obvious that the correlations for the extrema of the specific heat are better than those for the tunneling parameters. We will come back to this point in the next section. Finally it turns out that the $b_{i,\mathrm{exp}}$ agree very well with the simulated values $b_{i,\mathrm{sim}}$. Hence the physics of the LJ glasses as derived from our simulations *quantitatively* agrees with typical experimental data.

One might argue that the above results are just manifestations of some trivial correlations. For example the mere fact that the $T_{C,i}$ for SiO_2 are higher than those for, e.g., PS can be simply understood by the fact that silicate glasses are much stiffer than polymers, which is for example expressed by the higher glass transition temperature. However, obviously this picture breaks down in the case of LiCl-7H_2O which among all analyzed glasses has the smallest glass transition temperature but one of the highest values of $T_{C,2}$. Of course, the reason for this behavior is the strong dependence of $T_{C,i}$ on μ. In this sense the correlations in Figs. 4–7 contain much more information than guessed intuitively. To stress this point, we analyze the correlation of $T_{C,1}/T_g$ and $T_{C,2}/T_g$ with μ. The corresponding plot can be seen in Fig. 8. One can clearly see that the predicted behavior $T_{C,1}/T_g \propto \mu^{-2/3}$ and $T_{C,2}/T_g \propto \mu^{-1/2}$ is very well fulfilled. In principle the exponents c_i could have been derived directly from this plot with good accuracy. We see again that the internal energy scale as well as μ determine the temperature dependence of the specific heat.

The previous analysis indicates that to a large degree all

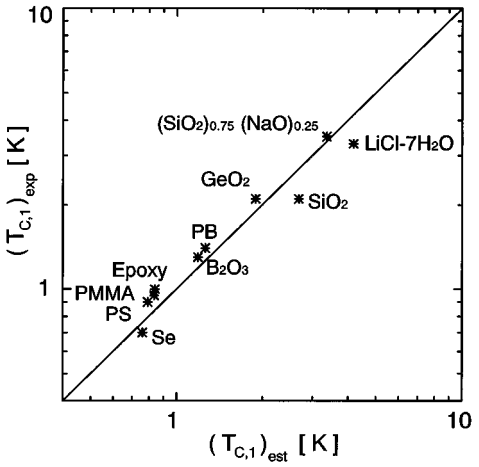

FIG. 6. The same analysis as in Fig. 4 for $T_{C,1}$.

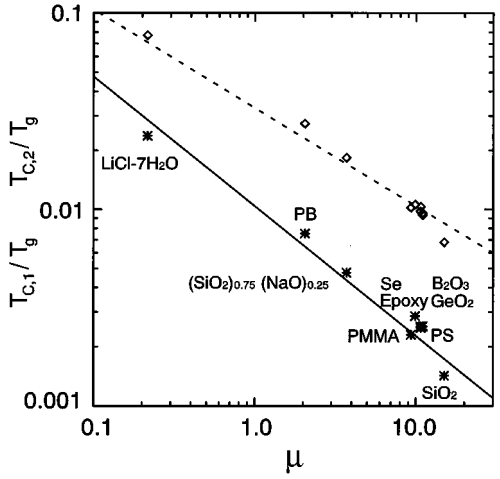

FIG. 8. A plot of $T_{C,1}/T_g$ and $T_{C,2}/T_g$ vs μ. The solid lines correspond to a scaling with $\mu^{-2/3}$ and $\mu^{-1/2}$, respectively.

TABLE III. The ratio of T_s and T_g for four glasses.

	T_s [K]	T_s/T_g	ω [MHz]	Ref.
SiO_2	45	0.03	20	29
LASF7	110	0.11	30	28
B_2O_3	83	0.16	20	29
GeO_2	170	0.20	20	29

low-temperature properties are independent of the microscopic structure. Hence it might be surprising that there exists another low-temperature parameter which cannot be analyzed in analogy to the quantities discussed until now. The temperature dependence of the absorption of sound displays a maximum around 30 K (for SiO_2), hence defining a temperature T_s. At these elevated temperatures the dynamics of the DWP's can already be described in classical terms[10] (however, see Ref. 17 for some recent aspects of the sound absorption). Since the relaxation of DWP's determines the sound absorption for these temperatures one can already conclude from dimensional arguments that $T_s \propto B \propto T_g$ if measured in approximately the same frequency region (T_s only depends logarithmically on frequency). In Table III we present for four glasses the values of T_s and T_s/T_g. Obviously the ratio T_s/T_g is far from being constant. This means that the temperature of the peak of sound absorption strongly depends on the microscopic structure of the glass. As mentioned before this finding is in agreement with the experimental observation that slight modifications of a glass may significantly alter the value of T_s.[17]

V. DISCUSSION

In the preceding section we analyzed the question whether or not the low-temperature parameters depend on the microscopic structure, and showed that there is only a weak dependence, so that all glasses can be mapped onto LJ glasses, at least for the low temperature data.

First we briefly want to discuss possible experimental uncertainties. The quantity $n_{\rm eff}\gamma^2/\rho v^2$ can be derived either from the plateau of the sound absorption, or from the temperature dependence of the sound velocity.[1] It turns out that for LASF-7, for example, both values vary by a factor of 2 indicating some experimental or theoretical inconsistencies.[28] However, in the work of Berret and Meissner, all glasses have been analyzed consistently so that the relative error should be smaller. Nevertheless we cannot exclude the possibility that the residual scattering in Figs. 4 and 5 is due partly to inconsistencies in the experimental data, like the one mentioned. In contrast, the extrema of $\hat{C}(T)$ can be reliably extracted from the temperature dependence of the specific heat. The same holds for the peak of the sound absorption.

Next we want to comment on the reliability of our numerical results. As we have shown in Sec. III the values of the exponents c_i can already be roughly estimated by the general properties of the p_i so that they are quite insensitive to numerical details. Hence all statements which are related to correlations and possible dependences on the microscopic structure can be deduced from very general arguments. In contrast, the prefactors $b_{i,\rm sim}$ strongly depend on details of our simulation and hence are sensitive to possible remaining uncertainties like those discussed in Sec. II. Although we do not stress the excellent agreement between the $b_{i,\rm sim}$ and the $b_{i,\rm exp}$, it clearly demonstrates the reliability of our results.

It is somewhat surprising that most of the low-temperature properties are insensitive to the exact microscopic structure, which implies that, e.g., silicate glasses or polymers are not very different from LJ glasses at low temperatures. Let us take as an example a simple polymer like PS and identify the monomers as generalized LJ atoms. One of the main differences between PS and a LJ glass is the fact that monomers not only interact by long-range forces but also by covalent forces which fix the distance of monomers along a polymer chain. However, from the systematic analysis of the microscopic structure of the DWP's we found (see Sec. III) that two adjacent atoms tend to keep their relative distance fixed during the transition between the two walls. Hence, additional forces fixing the distance of some atoms would only mildly effect the nature of the DWP's. Therefore the main structural difference between polymers and LJ glasses is not relevant for the nature of soft modes. Furthermore, one should keep in mind that a soft mode typically corresponds to collective motion of a number of adjacent units, implying an average over microscopic details. This argument is similar to the explanation of universal behavior near phase transitions where the correlation length far exceeds the microscopic length scale.[18]

The second argument implies that the degree of universality should be correlated with the effective mass p of the soft modes. This observation can be used to explain the different degrees of universality for the low-temperature parameters. As already discussed in Sec. III we expect SWP's to have much larger values of p than DWP's. Since the extrema of $\hat{C}(T)$ are related to the energy distribution of SWP's it is not surprising that the degree of universality is very high for $T_{C,1}$ and $T_{C,2}$. In contrast, the values of γ, $n_{\rm eff}\gamma^2$, and T_s depend on the properties of DWP's. It has been shown for SiO_2 that the relaxational behavior near T_s is dominated by DWP's with barrier heights of the order of 500 K.[10] It is easy to check from application of the WKB formula that potentials with barrier heights of this order have negligible tunneling matrix elements.[1] Stated differently, at temperatures near 1 K only DWP's with significantly smaller barrier heights are relevant. According to our simulations (see Fig. 2) this implies that DWP's relevant for the sound absorption near T_s are much more localized than those which are important at 1 K. This argument explains why the degree of universality for γ and $n_{\rm eff}\gamma^2$ is still rather high whereas there is no universal behavior at all for T_s.

We would like to mention that at higher temperatures also a different kind of DWP may occur. MD simulations at elevated temperatures have shown that it is possible the adjacent soft modes merge together and form extended soft modes which can probably be decomposed into a few more localized soft modes.[13] They are not included in our statistical analysis.

It has been pointed out in literature that the height of the bump of $\hat{C}(T)/T^3$ is related to the fragility of glasses.[8] This has been interpreted to mean that the ratio of SWP's to

DWP's is larger for strong glasses. Since this ratio is determined by the parameter A_3, we expect A_3 to be smaller for strong glasses. Most strong glasses are network glasses which tend to stabilize the soft modes. Since the value of w_3 is a measure for the instability of the corresponding soft mode it is consistent that strong glasses typically have lower values of w_3. On the basis of our analysis we are in a position to check whether there are additional correlations of the low-temperature properties with the fragility of glasses. The strongest glasses analyzed in Figs. 6 and 7 are SiO_2 and GeO_2. No anomalous behavior with respect to their values of $T_{C,1}$ and $T_{C,2}$ can be observed. Therefore we can conclude that in contrast to A_3 the values of A_2 and A_4 are not significantly correlated with the fragility.

We believe that the number of glasses analyzed is large enough to be able to identify some generic behavior of structural nonmetallic glasses at low temperatures. This implies that for any major deviations one should be able to point out microscopic peculiarities. One example for glasses which do not follow the standard behavior are glasses which form a very strong tetrahedral network like $Se_{60}Ge_{40}$.[30] It turns out that the deformation potential is more than twice as small as expected from the correlation expressed in Fig. 4. This can be understood from our analysis of the deformation potential. As already mentioned, the value of the deformation potential is generally larger for glasses with strong disorder. We showed in Ref. 21 that for LJ glasses with approximate icosahedral symmetry around a DWP the corresponding deformation potential strongly decreases. We have checked that similar arguments hold for tetrahedral symmetry. A detailed analysis of this problem is beyond the scope of the paper. The disorder of a network glass is somewhat reduced compared to a fragile glass, perhaps explaining why the deformation potential of strong tetrahedral network glasses is smaller than expected. We also observed that the simulated and experimental extrema of the specific heat of glycerole[6] differ by a factor of 2. This seems to indicate that the hydrogen bonds somewhat influence the low-temperature properties.

We should note that near the temperature $T_{C,2}$ the interaction between the soft modes starts to dominate the dynamics. It has been proposed that this effect is responsible for a decrease of $\hat{C}(T)$ with further increasing temperature.[7,31] As outlined above, the occurrence of the maximum in the specific heat $\hat{C}(T)$ can be also be explained on the basis of the distribution of soft modes. Unfortunately, both explanations for the occurrence of the maximum yield the same μ dependence of $f_4(\mu)$. Therefore we cannot distinguish between both mechanisms.

Recently, Parshin has extensively applied the SPM to the explanation of the low-temperature properties. Although his approach has some similarities with our analysis we would like to stress some significant differences. First, in contrast to the phenomenological approach of the SPM our analysis started from a microscopic description of the glass. This allowed us to determine the low-temperature parameters in a quantitative way. Second, for the estimation of n_{eff} and γ Parshin used the atomic mass as a value for m rather than the molecular mass. Therefore it is not surprising that he still obtains large deviations between the estimations and the actual experimental values. As shown above a more convenient way for any quantitative analysis is to introduce the glass transition temperature as the appropriate internal energy scale. Third, he relates the similarity of the low-temperature parameters for many glasses to the interaction of the soft modes. In a different context this argument has been already put forward.[32,33] In contrast, we believe that this universality can be explained without postulating a strong interaction. Rather it is the collective dynamics of several adjacent molecules or atoms which to first approximation reduce any dependences on the microscopic structure.

VI. SUMMARY

We have presented an extensive analysis of the low-temperature properties of glasses. In the first step we obtained the low-temperature Hamiltonian of a LJ glass largely from a systematic analysis of simulated glasses. The main ingredient is a systematic search routine for DWP's. In this way we can extract important information about the statistics of the DWP's, the geometric properties of the DWP's, the coupling of the DWP's to the phonon bath, and the relation of the size of the DWP's to its energy parameters. This step can be viewed as a microscopic derivation of the standard tunneling model and the soft potential model. In a second step we expressed the low-temperature parameters of LJ glasses in terms of macroscopic parameters (ρ, v, T_g). Finally we applied this formalism to the estimation of the low-temperature parameters of more general glasses. The deviations from experimental data can be used as a measure for the relevance of the individual microscopic structure. A quantitative analysis of the deviations reveals that apart from the peak of sound absorption all low-temperature properties are only mildly influenced by the individual microscopic structure. Hence it is possible to speak of a universal low-temperature behavior in a quantitative sense. It is not only the mere existence of phenomena like the bump of the specific heat bath also the *absolute* values of the low-temperature parameters which, after appropriate scaling, are approximately identical for many different glasses. Furthermore it turns out that the degree of universality is determined by the spatial extension of the relevant soft modes. This is in agreement with intuition and directly explains why the peak of sound absorption is much more sensitive to microscopic variations of the glass than, e.g., the number of DWP's.

ACKNOWLEDGMENTS

We greatly acknowledge fruitful discussions with D. Dab, S. Hunklinger, D. A. Parshin, and H. W. Spiess, and financial support from the NSF.

[1] W. A. Phillips, Rep. Prog. Phys. **50**, 1657 (1987).
[2] W. A. Phillips, J. Low Temp. Phys. **7**, 351 (1972).
[3] P. W. Anderson, B. I. Halperin, and C. M. Varma, Philos. Mag. **25**, 1 (1972).
[4] V. G. Karpov, M. I. Klinger, and F. N. Ignatiev, Zh. Eksp. Teor. Fiz. **84**, 760 (1983) [Sov. Phys. JETP **57**, 439 (1983)].
[5] U. Buchenau, Yu. M. Galperin, V. L. Gurevich, and H. R. Schober, Phys. Rev. B **43**, 5039 (1991).
[6] L. Gil, M. A. Ramos, A. Bringer, and U. Buchenau, Phys. Rev. Lett. **70**, 182 (1993).
[7] D. A. Parshin, Phys. Rev. B **49**, 9400 (1994).
[8] A. P. Sokolov, E. Rössler, A. Kisliuk, and D. Quitmann, Phys. Rev. Lett. **71**, 2062 (1993).
[9] *Amorphous Solids–Low-Temperature Properties*, edited by W. A. Phillips (Springer, Berlin, 1981).
[10] D. Tilebürger, R. Merz, R. Ehrenfels, and S. Hunklinger, Phys. Rev. B **45**, 2750 (1992).
[11] P. Reichert and R. Schilling, Phys. Rev. B **32**, 5731 (1985).
[12] W. Uhler and R. Schilling, Phys. Rev. B **37**, 5787 (1988).
[13] H. R. Schober, C. Oligschleger, and B. B. Laird, J. Non-Cryst. Solids **156-158**, 965 (1993).
[14] B. B. Laird and H. R. Schober, Phys. Rev. Lett. **66**, 636 (1991).
[15] H. R. Schober and B. B. Laird, Phys. Rev. B **44**, 6746 (1991).
[16] A. Heuer and R. J. Silbey, Phys. Rev. Lett. **70**, 3911 (1993).
[17] S. Rau, C. Enss, S. Hunklinger, P. Neu, and A. Würger, Phys. Rev. B **52**, 7179 (1995).
[18] S. K. Ma, *Statistical Mechanics* (World Scientific, Singapore, 1987).
[19] A. Heuer and R. J. Silbey, Phys. Rev. B **49**, 1441 (1994).
[20] T. A. Weber and F. H. Stillinger, Phys. Rev. B **32**, 5402 (1985).
[21] A. Heuer and R. J. Silbey, Phys. Rev. B **48**, 9411 (1993).
[22] D. Dab, A. Heuer, and R. J. Silbey, J. Luminesc. **64**, 95 (1995).
[23] D. A. Parshin and S. Sahling, Phys. Rev. B **47**, 5677 (1993).
[24] A. Heuer and H. W. Spiess, J. Non-Cryst. Solids **176**, 294 (1994).
[25] F. A. Lindemann, Z. Phys. **11**, 609 (1910).
[26] *Proceedings of the International Discussion Meeting on Relaxation in Complex Systems II* [J. Non-Cryst. Solids **172-174**, (1994)].
[27] J. F. Berret and M. Meissner, Z. Phys. B **70**, 65 (1988).
[28] J. F. Berret, J. Pelous, R. Vacher, A. K. Raychaudhuori, and M. Schmidt, J. Non-Cryst. Solids **87**, 70 (1986).
[29] J. T. Krause and C. R. Kurkjian, J. Am. Ceram. Soc. **51**, 226 (1968).
[30] J. Y. Duquesne and G. Bellessa, Philos. Mag. B **52**, 821 (1985).
[31] V. L. Gurevich, D. A. Parshin, J. Pelous, and H. R. Schober, Phys. Rev. B **48**, 16 318 (1993).
[32] C. C. Yu and A. J. Leggett, Comments Condens. Matter Phys. **14**, 231 (1988).
[33] A. J. Leggett, Physica B **169**, 322 (1991).
[34] S. Kelham and H. M. Rosenberg, J. Phys. C **14**, 1737 (1981).
[35] J. E. Graebner, B. Golding, and L. C. Allen, Phys. Rev. B **34**, 5696 (1986).
[36] G. K. White, J. A. Berch, and M. H. Manghnani, J. Non-Cryst. Solids **23**, 99 (1977).
[37] R. C. Zeller and R. O. Pohl, Phys. Rev. B **4**, 2029 (1971).
[38] J. J. Freeman and A. C. Anderson, Phys. Rev. B **34**, 5684 (1986).
[39] G. K. White, S. J. Collocott, and J. S. Cook, Phys. Rev. B **29**, 4778 (1984).